Accepted Manuscript

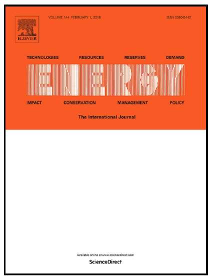

Numerical simulation on thermoelectric and mechanical performance of annular thermoelectric generator

Shifa Fan, Yuanwen Gao

PII:	S0360-5442(18)30358-X
DOI:	10.1016/j.energy.2018.02.124
Reference:	EGY 12424
To appear in:	*Energy*
Received Date:	16 November 2017
Revised Date:	25 January 2018
Accepted Date:	21 February 2018

Numerical simulation on thermoelectric and mechanical performance of annular thermoelectric generator

Shifa Fan, Yuanwen Gao*

Key Laboratory of Mechanics on Western Disaster and Environment with the Ministry of Education, Lanzhou University;

College of Civil Engineering and Mechanics, Lanzhou University, Lanzhou 730000, China

*Corresponding author Yuanwen Gao

Email: ywgao@lzu.edu.cn

Tel: (0086) 931 8914560; Fax: (0086) 931 8914561

Abstract: In this paper, a three dimensional finite element model of annular thermoelectric devices is established to optimize the geometric dimensions and the number of thermocouples for the enhancement of the thermoelectric performance and mechanical reliability. The influences of geometric dimensions and the number of the thermocouples on the thermoelectric performance and the mechanical reliability of annular thermoelectric generators are investigated, respectively. The numerical results indicate that with the increasing the angle ratio of the thermoelectric leg, the maximum von Mises stress in the legs of thermocouples decreases first and then increases, and the thermoelectric performance of the annular thermocouple can be significantly improved. In addition, increasing the length of legs of thermocouples would reduce the thermoelectric performance, but improve the mechanical reliability of annular thermocouples. For the whole annular thermoelectric generator, there exists different optimal number of thermocouples to enhance the thermoelectric performance for different external resistance. The number of thermocouples has little influence on the maximum von Mises stress in the legs of annular thermoelectric generators. Finally, the optimal geometric dimensions of the annular thermoelectric generator with high thermoelectric and mechanical performance are also discussed. These results can provide some guidance for the optimization design of annular thermoelectric generators.

Key word: the geometric dimensions, the thermoelectric performance, the mechanical reliability, annular thermoelectric generator

Nomenclature	
$\mathbf{a}$	vector of thermal expansion coefficient, K^{-1}

C_V	volumetric heat capacity, Jm^{-3}·K^{-1}
CTE	coefficient of thermal expansion, K^{-1}
$[D]$	stiffness matrix, N m^{-1}
E	Young's modulus, GPa
$\mathbf{E}$	electric field intensity vector, V m^{-1}
$\mathbf{f}$	volume force, N m^{-3}
I	electric current, A
$\mathbf{J}$	current density vector, A m^{-3}
L	length of thermoelectric leg in annular thermoelectric generator, m
P	output power of the annular thermoelectric generator, W
$\mathbf{q}$	heat flux vector, W m^{-2}
$\dot{\mathbf{q}}$	heat generation rate per unit volume, W m^{-3}
Q	heat- flow density, J m^{-2}
Q_{in}	absorbed heat in the hot end of the annular thermoelectric generator, W
R_L	external load resistance, Ω
$\mathbf{S}$	stress vector, Pa
T	temperature, K
$\mathbf{u}$	displacement vector, m
α	Seebeck coefficient, V K^{-1}
$\boldsymbol{\varepsilon}$	strain vector
η	conversion efficiency
θ	angle ratio of the thermoelectric leg
λ	thermal conductivity, W m^{-1}K^{-1}
μ	Poisson's ratio
$\boldsymbol{\rho}$	density vector, Kg m^{-3}
σ	electrical conductivity, Ω^{-1}m^{-1}
φ_1	angle of a single thermoelectric leg, degree
φ_2	a half of the angle between two legs, degree
φ	total angle, degree

1. Introduction

With the development of human society, the renewable and environmentally friendly energy conversion technology has become a hot topic due to the aggravation of environmental pollution and the decrease of fossil energy. In the traditional energy conversion processes, more than 50 % of energy [1] is emitted as wasted heat into environment, especially in vehicles. However, converting some wasted heat into electricity can not only increase the efficiency of energy conversion, but also reduce the use of fossil fuel. As one of the potential energy converters, thermoelectric devices can convert heat energy into electricity directly, which is widely used in the recovery of vehicle waste heat and solar energy etc., due to its safety, low maintenance cost and zero emission etc.[2-7].

In practical applications, there is an urgent need for high conversion efficiency and output power of thermoelectric devices. The efficiency and output power of thermoelectric device significantly depend on the merit value of thermoelectric materials and temperature difference between the hot side and cold side of the legs [6, 8-11]. Ali et al. [8] used the thermoelectric materials with higher merit value in the hot side to improve the performance of the thermoelectric generator, their results showed that the power output and efficiency of the segmented thermoelectric generator is higher than those of thermoelectric generator with single material. In order to increase the temperature difference between the two sides of the thermoelectric device, Omer and Infield [9] designed a two stage solar concentrator, which not only improves the stability and efficiency of the thermoelectric device, but also enhances the light-gathering efficiency. In addition, an analytical model of high efficiency segmented thermoelectric generator was proposed and formulated by Hadjistassou and Kyriakides [11], they found that the peak efficiency of the segmented thermoelectric generator could reach 5.29% when the temperature difference is 324.6K. Meanwhile, geometric size of thermoelectric devices is also an important factor for the thermoelectric performance [12-16].The multi-objective optimization of a thermoelectric device was investigated by Ibrahim et al. [12], they proposed a unique configuration of the thermoelectric generator, which has the high thermal efficiency and output power simultaneously. The optimization of the slenderness ratio and external load on the performance of traditional thermoelectric generator was discussed by Yilbas and Sahin [13], they found that the efficiency is high for the slenderness ratio less than 1 at the fixed external load. Later, Sahin and Yilbas [14] investigated the influence of the leg geometry on the performance of the thermoelectric generator, and found that the efficiency of the pin thermoelectric generator is higher than that of the traditional thermoelectric generator. The structural optimization of two-stage thermoelectric generators was discussed by Liu et al. [15]. They used the simplified conjugate-gradient method to optimize three geometric parameters for improving the power output and conversion efficiency simultaneously. Rezania et.al [16] explored the effect of footprint ratio of n- and p-type thermoelectric legs on the performance of thermoelectric devices, their results illustrated that the max power generation occurs where the footprint ratio is less than 1. From above literatures, it is noted that the effect of geometric dimensions on the thermoelectric performance of thermoelectric devices is very significant. Compared to the traditional flat thermoelectric generator, the heat transfer in the cold and hot ends of the annular thermoelectric generator can be improved because of larger heat transfer area and its cylindrical structure, Kumar et.al [17] found that the power generation in the cylindrical design is larger than the traditional designs in their investigation. Therefore, it has great application prospect in solar energy, automobile exhaust gas recovery, space (radioisotope thermoelectric generators) and other fields [17-19]. Some researchers [19-21] have established the one-dimensional theoretical model to study the influence of the ratio of internal and external radius on the performance of the annular thermoelectric generator, however, few researchers pay attention to study the influence of angle ratio of leg in the thermoelectric performance of annular thermoelectric devices, especially in the case of three-dimension.

In addition, the thermoelectric generators always work in a temperature difference environment, resulting in the thermal stress caused by the different thermal expansion of components, and excessive stress can reduce the service life of thermoelectric generators. Therefore, more and more researchers have been attracted to the study on the mechanical reliability of thermoelectric generators in recent years [22-27]. The influence of various leg geometries on the thermoelectric and thermo-mechanical performance of thermoelectric devices was analyzed by Erturun et al. [22], their results showed that the thermal stress levels in the trapezoidal and cylindrical legs are smaller than that in the rectangular legs. Wu et al. [23] simulated numerically the thermal stress of a thermoelectric power generator, they found that appropriate thickness of ceramic plate and soldering layer can reduce the thermal stress level effectively. Based on the Skutterudite and Bismuth-Telluride materials, Jia and Gao [24] obtained the optimal structural design of the segmented thermoelectric generator to enhance the thermoelectric and mechanical performance. Gao et al [25] investigated the thermal stress distribution of a thermoelectric generator based on the anisotropic properties and obtained the better mechanical performance of thermoelectric generator by optimizing the structural parameters. As above motioned, the influence of the structure parameters on the mechanical performance is significant, and the relationship between thermoelectric performance and stress levels is inverse in the thermoelectric generator [25]. Moreover, the mechanical reliability of annular thermoelectric devices has not been studied systematically, therefore, it is desired to investigate the effect of the structural parameters on the thermoelectric and mechanical performance of the annular thermoelectric generator.

In this study, a three dimensional finite element model of annular thermoelectric device is established to investigate the thermoelectric performance and mechanical reliability. In order to simplify the model and save time, the single thermocouple is established to discuss the influence of the angle ratio and length of the thermoelectric legs on the thermoelectric performance and mechanical reliability firstly, and then the influence of the number of thermocouples on the thermoelectric performance and mechanical reliability of the whole annular thermoelectric generator is studied. Finally, the optimal geometric dimensions of the annular thermoelectric generator with high thermoelectric and mechanical performance is also obtained and discussed. These results are expected to be helpful in the design of actual annular thermoelectric generators.

The rest of this paper is organized as follows. First of all, the physical model and governing equations of the annular thermoelectric device is presented in the Section 2. Then the influence of structure parameters on the performance of annular thermoelectric generators is investigated in the Section 3. Finally, some useful conclusions are summarized in Section 4.

2. Model description

2.1 Physical model

A thermoelectric device investigated in the paper is presented in Fig. 1, including the thermally conducting and electrically insulating ceramic plates, the conducting copper, the welding layer and annular thermoelectric legs. In this figure, φ_1 represents the angle of a single thermoelectric leg, and φ_2 represents a half of the angle between two legs. The basic parameters of the model are listed in Table I. In addition, the Bi_2Te_3 is selected as the thermoelectric materials, and the yielding stress of Bi_2Te_3 is 112MPa [28]. The thermoelectric properties of Bi_2Te_3 are presented in the Fig.2, the other material properties in the simulation are listed in Table II. The copper and welding layer are considered as the elastoplastic materials, the yielding stress, tangential modulus of copper and welding layer are 70 MPa, 24 GPa and 26 MPa, 8.9 GPa, respectively[23].

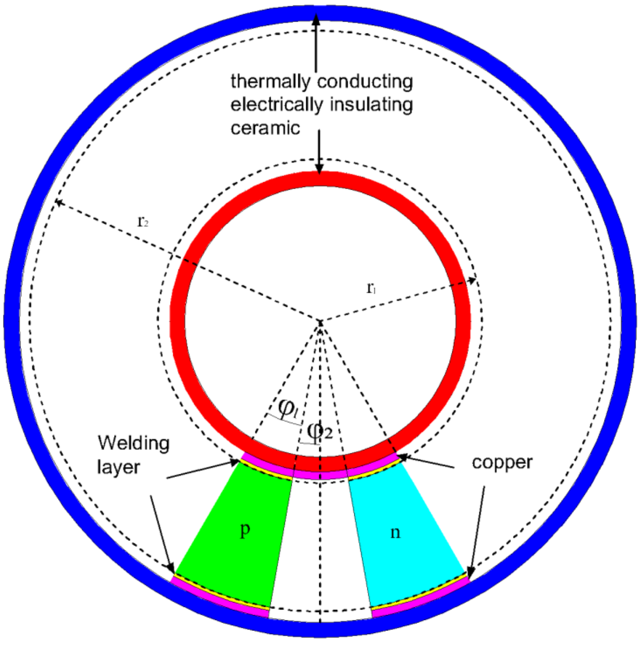

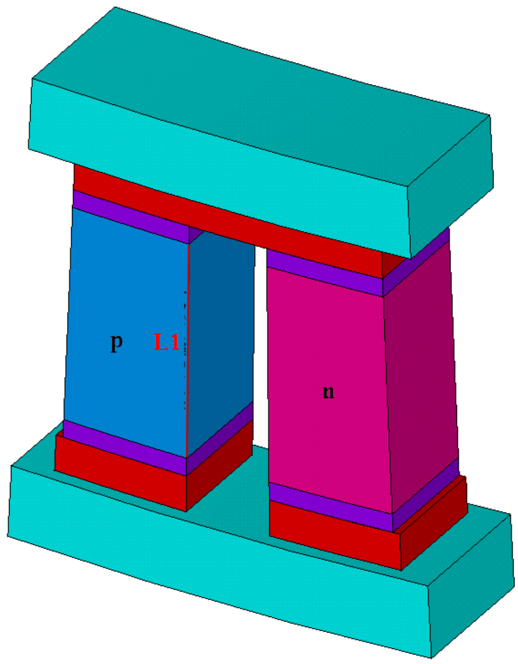

Fig.1 the structure diagram (a) and the three-dimensional view (b) of the annular thermoelectric generator

Table I geometry parameters of the annular thermoelectric generator

	Length (mm)	Thickness (mm)	Inner radius (mm)	$\Delta\varphi$
Ceramic	0.5	1	25	
Wielding layer	0.125	0.8	---	
Copper	0.25	0.8	---	Depend on study case
p-Bi_2Te_3	Depend on study	0.8	---	
n-Bi_2Te_3	Depend on study	0.8	---	

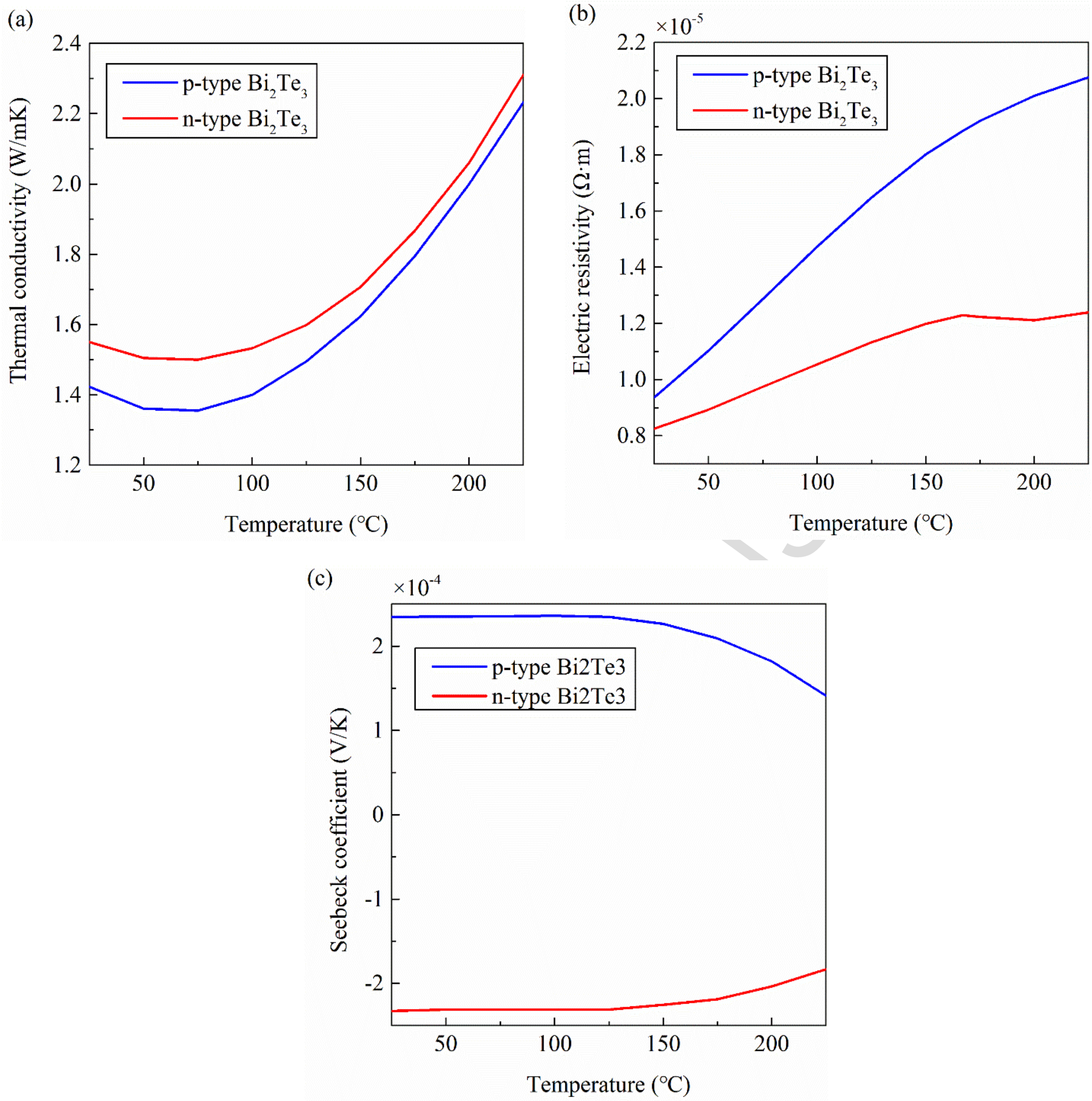

Fig. 2 thermoelectric properties for the Bi2Te3 materials [29] (a) thermal conductivity (b) electric resistivity (c) seebeck coefficient.

Table II the properties of the materials used in this paper [25].

	CTE (k^{-1})	ρ (kg/m^3)	C_V (J/(kg·K))	E (GPa)	μ	λ (W/mK)	σ ($\Omega^{-1}\cdot m^{-1}$)
Ceramic	0.68e-5	3970	800	340	0.22	25	1e-12
Wielding layer	2.7e-5	7240	210	44.5	0.33	55	2e7
Copper	1.7e-5	8930	386	120	0.3	385	5.9e7
Bi_2Te_3	0.8e-5~1.32e-5	7740	154.4	65-59	0.23	---	---

For the annular thermoelectric generator, the geometric dimensions have obvious influence on the thermoelectric performance [20], therefore, in order to investigate the effect of the geometry dimensions on the thermoelectric and mechanical performance, the angle ratio θ of the thermoelectric leg is defined as:

$$\theta = \varphi_1 / \varphi \tag{1}$$

where $\varphi = \varphi_1 + \varphi_2$ represents the total angle, which equals to half-angle of the single thermocouple, in addition, the length of the thermoelectric leg in the annular thermoelectric generator is defined as:

$$L = r_2 - r_1 \tag{2}$$

where r_1 and r_2 stand for the inner and outer radius of the annular thermoelectric generator (shown in Fig. 1(a)).

2.2 Thermoelectric and thermal stress analyses

The physical process in the thermoelectric system involves the Peltier effect, Thomson effect, irreversible Joule and Fourier effects, which are taken into account in our model. The steady-state governing equation of the heat flow is expressed as [24]:

$$\nabla \cdot \mathbf{q} = \dot{q} \tag{3}$$

where $\mathbf{q}$ and $\dot{q}$ stand for the heat flux vector and the heat generation rate, respectively. The governing equation of electric charge can be expressed as [24]:

$$\nabla \cdot \mathbf{J} = 0 \tag{4}$$

in which $\mathbf{J}$ is the current density vector. The coupled thermoelectric equations can be expressed as [22]:

$$\begin{cases} \mathbf{q} = \alpha T \mathbf{J} - \lambda \nabla T \\ \mathbf{J} = \sigma(\mathbf{E} - \alpha \nabla T) = -\sigma(\nabla \varphi_e + \alpha \nabla T) \end{cases} \tag{5}$$

where α, T, λ and σ are the Seebeck coefficient, temperature, thermal conductivity and electric conductivity, respectively. $\mathbf{E}$ is electric field intensity vector, which can be expressed by an electrical potential φ_e, that is $\mathbf{E} = -\nabla \varphi_e$.

Substituting Eq. (5) into Eqs. (3) and (4), the thermoelectric coupled governing equations can be rewritten as follows:

$$\begin{cases} \nabla \cdot (\alpha T \mathbf{J}) - \nabla \cdot (\lambda \nabla T) = \dot{q} \\ \nabla \cdot (\sigma \nabla \varphi_e) + \nabla \cdot (\sigma \alpha \nabla T) = 0 \end{cases} \tag{6}$$

In addition, the annular thermoelectric devices are operated in a temperature-difference condition, the thermal mismatch for different materials can cause the thermal stress in the annular thermoelectric generator. Thus, the deformation and the temperature field interact each other. The mechanical equilibrium governing equations and strain-displacement relations for the thermoelectric devices can be expressed as [24]:

$$[A]\mathbf{S}+\mathbf{f}=0 \tag{7}$$

$$\boldsymbol{\varepsilon}=[A]\mathbf{u} \tag{8}$$

where $[A]$ stands for the differential operator about the mechanical equilibrium. $\mathbf{S}$ and $\boldsymbol{\varepsilon}$ are the stress vector and strain vector respectively, $\mathbf{f}$ is the volume force, $\mathbf{u}$ is the displacement vector. The thermal-mechanical coupling constitutive equations of the thermoelectric device can be expressed as [30]:

$$\mathbf{S}=[D]\boldsymbol{\varepsilon}-\boldsymbol{\beta}\Delta T \tag{9}$$

$$Q=T_0\boldsymbol{\beta}^T\boldsymbol{\varepsilon}+\rho C_V\Delta T \tag{10}$$

where $[D]$ stands for the stiffness matrix, $\boldsymbol{\beta}$ is the thermo-elastic coefficient vector, which satisfies the relation: $\boldsymbol{\beta}=[D]\mathbf{a}$, $\mathbf{a}$ is the thermal expansion coefficient vector. Q is the heat-flow density, T_0 is the reference Kelvin temperature and C_V is the volumetric heat capacity.

The above equations can describe the coupling thermal, electrical and mechanical behaviors of thermoelectric device. However, because of the temperature dependent properties of materials, it is difficult to obtain the analytical results directly. Thus, a finite element formulas is given here by the variational principle with these equations

2.3 The calculation method

Boundary conditions and some reasonable assumptions are listed as follows, the simplified model is easy to deal with, while without too much deviation from the real conditions:

(a) Heat radiation and convection on all surfaces are ignored.

(b) All the surfaces except the hot and cold ends are supposed to be heat insulation.

(c) Both electrical and thermal contact resistances are neglected.

(d) The hot and cold ends of the annular thermoelectric generator are fixed at the values of 225°C and 25°C respectively.

(e) The reference voltage applied to the copper strip connected to the cold end of p-leg is zero.

(f) Suppose that the hot end of the annular thermoelectric generator is clamped, and the other boundaries are free.

The commercial software ANSYS is used to simulate the thermoelectric and mechanical performance of the annular thermoelectric generator under steady-state condition. The 20-node coupling element SOLID226 is selected, the general circuit element CIRCU124 is used to define the load resistance.

In addition, for the thermoelectric analysis, if the external load resistance R_L is given in advance, the output power P and the conversion efficiency of thermoelectric devices can be expressed as follows [24]:

$$P = I^2 R_L \tag{11}$$

$$\eta = P/Q_{\text{in}} \tag{12}$$

where I is the electric current, Q_{in} is the heat absorbed in the hot end. Both of them can be obtained by calculating the Eq. (6).

3. Results and discussion

3.1 Verification of the computational model

In order to verify the mesh convergence of the finite element approach employed, some numerical tests are conducted and the results are presented in Fig.3. In this figure, the N stands for the number of meshes on the path L1

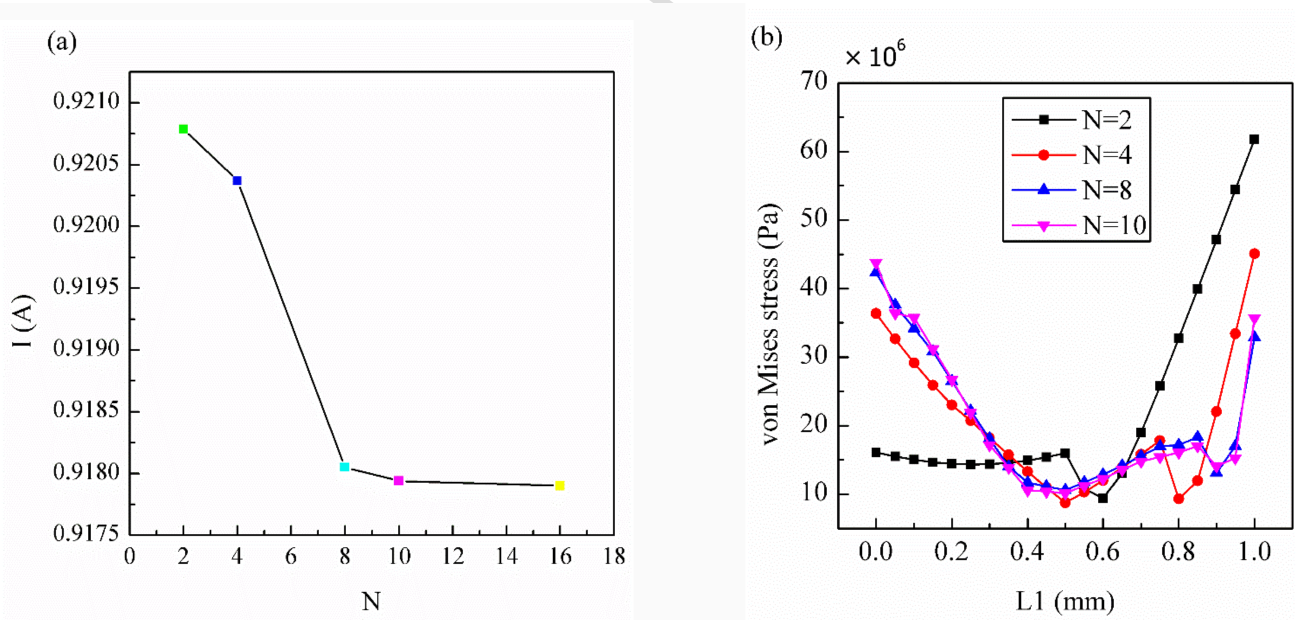

Fig.3 mesh convergence study for the calculated model at the boundary conditions used in this paper: (a) the current in thermoelectric analysis, (b) the von Mises stress in the thermal stress analysis.

(please see Fig. 1(b)). From the Fig. 3(a), it can be noted that the currents has little changed when N larger than 8, the difference of currents when N equals to 8 and 10 only accounts about 0.012% of that for $N = 10$. In the thermal stress analysis, the von Mises stress along the path L1 is showed in Fig. 3(b). It can be seen that the two curves are almost coincident when N equals to 8 and 10, and the difference of two cases only accounts 0.48% of the von Mises stress for $N=10$. Therefore, $N=10$ is selected as the number of meshes on the path L1 in the numerical code after considering the mesh convergence and computing time of the calculated model simultaneously.

To further validate the correct of our finite element model and the numerical code, we conducted a numerical test which is presented in [23]. The same parameters and conditions are reset as the previous study [21]. The comparison of results of our model and that of [23] is shown in Fig.4, it is obvious that the results are in good agreement. Which indicates that our model is reasonable and the numerical code is effective and accurate.

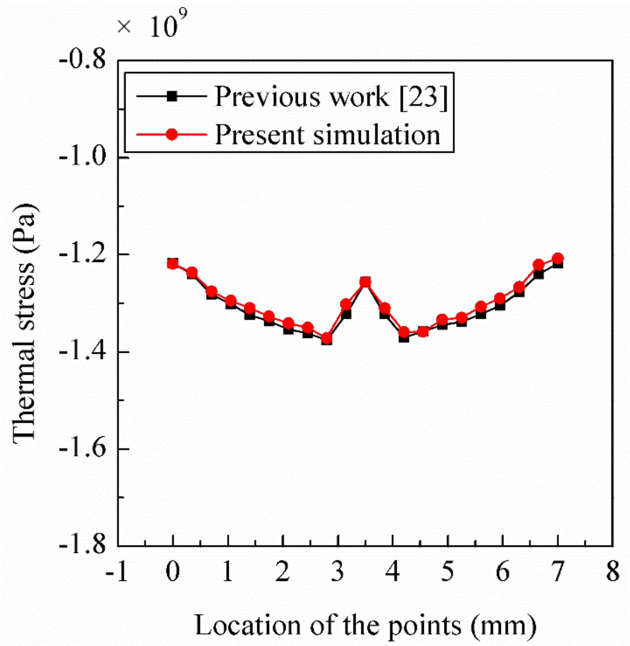

Fig. 4 validation of the present simulation with previous work [23]

3.2 The influence of angle ratio of the thermoelectric leg

The effect of the angle ratio of thermoelectric leg on the thermoelectric performance of the annular thermocouple is presented in Fig. 5. From Fig.5 (a) and (b), it is easy to see that both the output power density and conversion efficiency of the annular thermocouple increase with the increase of the angle ratio of the thermoelectric leg when the length of the thermoelectric leg is fixed (i.e. $L=1\mathrm{mm}$). The output power density and conversion efficiency have opposite trends with the increase of the length of the thermoelectric leg when the angle ratio of the thermoelectric leg is fixed (i.e. $\theta=0.9$). In this figure, the maximum of the output power density is 11.489×10^6 W/m^3, and the maximum conversion efficiency is 4.69% for $L=1\mathrm{mm}$, the results are consistent with the previous research findings of Shen et al. [17]. In the Fig.5 (c) and (d), it can be found that the output power density and conversion efficiency increase with

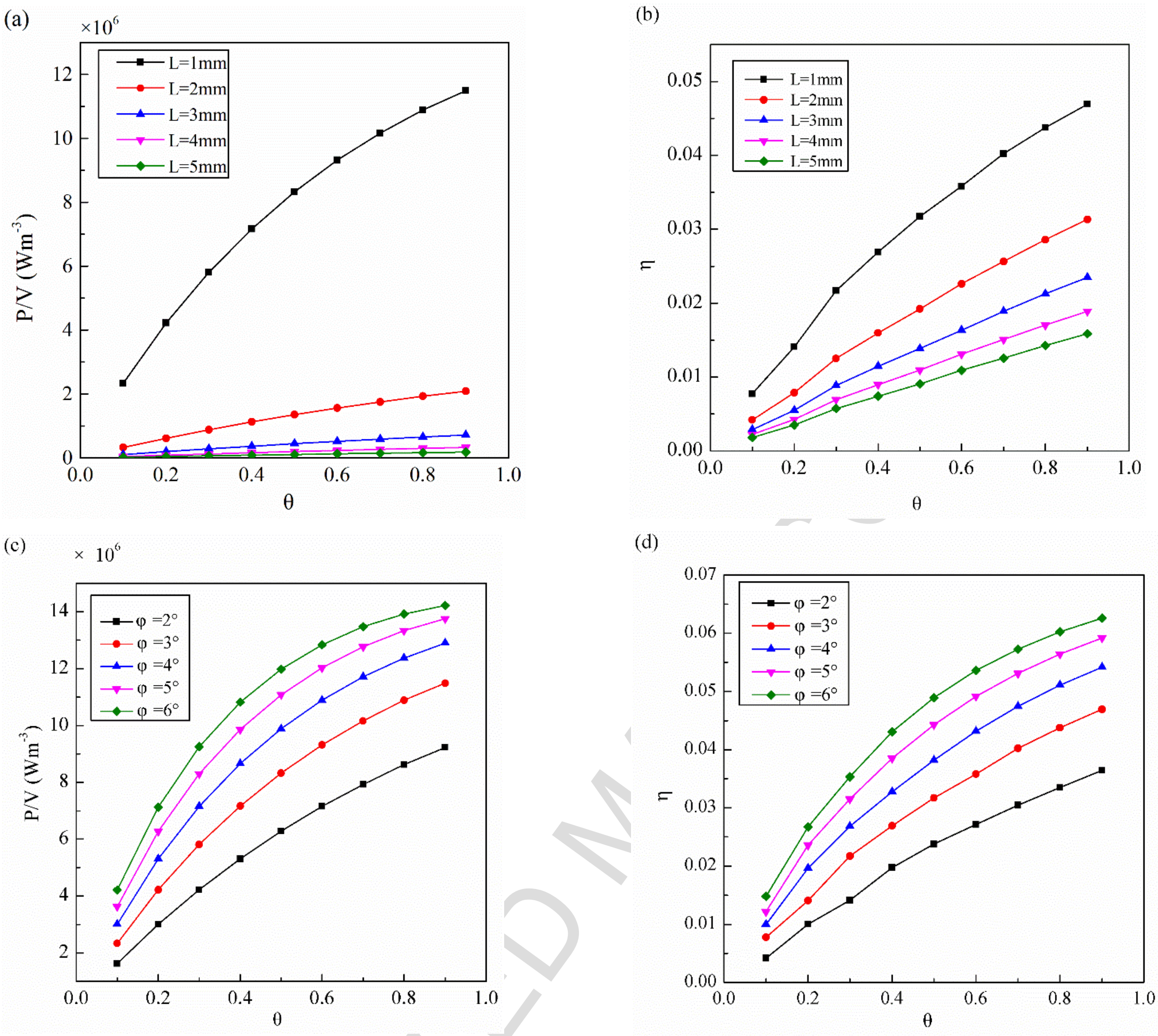

Fig.5 the effect of θ on the power output density (a, c) and the conversion efficiency (b, d) of the annular thermocouple when $R_L = 10\text{m}\Omega$, (a, b) $\varphi=3^{\circ}$, (c, d) $L=1\text{mm}$

increasing angle ratio of the thermoelectric leg at the fixed total angle (i.e. $\varphi=3^{\circ}$), the thermoelectric performance has identical trends with the increase of the total angle at the fixed angle ratio (i.e. $\theta=0.7$). All these indicate that just from the view for improving the thermoelectric performance, one can choose the dimensions that the angle ratio of the thermoelectric leg tends to 1.

Fig. 6 shows the effect of angle ratio of the thermoelectric leg on the mechanical performance of the annular thermocouple. From the Fig. 6(a), it can be seen that the maximum von Mises stress in the legs first decreases and then increases with the increase of the angle ratio of the thermoelectric leg for any different L. It can be found that the maximum von Mises stress is lowest for any L when the angle ratio is about 0.7. Here, we take the case ($L=1\text{mm}$) as an example, it can be seen that the maximum von Mises stress is 86.3MPa at $\theta=0.7$, it is reduced by 32.6% and

5.7% than that at θ=0.1 and θ=0.9 respectively, which will effectively improve the mechanical reliability of annular thermocouples. The maximum von Mises stress in legs exceeds the yielding stress when the angle ratio is less than 0.3 for L=1mm, which may reduce the service life of the annular thermocouple, even damage the device. In addition, when the angle ratio is fixed (i.e. θ=0.1), the maximum von Mises stress in the legs decreases with the increase of the length of the thermoelectric leg, which means that the thermoelectric performance of single annular thermocouples with shorter legs is better (as shown in Fig.5), but the mechanical reliability is poorer than that of annular thermocouples with longer legs. Nevertheless, for θ=0.7, the maximum von Mises stress of legs when L=1mm is only 3.7% higher than that when L=5mm, which implies that the mechanical performance of annular thermocouples with shorter legs is almost as same as that of annular thermocouples with longer legs when θ=0.7.

In the Fig.6 (b), it can be seen that there is always a minimum of the maximum von Mises stress in the legs by changing the angle ratio of the leg for any different φ, and the optimal angle ratio of the legs decreases with increasing the total angle for the mechanical performance of annular thermocouples. In addition, the maximum von Mises stress in the legs exceeds the yielding stress when the angle ratio is smaller than 0.2 or larger than 0.7 for φ=6°, which means the annular thermocouple may be damaged when the angle ratio is too large or too small. In the figure, when $\theta < 0.4$, the maximum von Mises stress of the legs decreases with increasing the total angle for the fixed angle ratio of the leg (i.e. $\theta = 0.3$); when $\theta \geq 0.7$, the maximum von Mises stress in the legs of annular thermocouples, firstly, decreases to the minimum value, then increases with the increase of total angle of the legs for the fixed angle ratio (i.e. θ=0.7, as shown in Fig. 6(c)). Moreover, from the Fig. 6(b) and (c), it is evident that the maximum von Mises stress in the leg of annular thermocouples achieves the minimum when the θ=0.7, φ=3°.

In addition, the variation of the maximum von Mises stress in the legs of annular thermocouples with the temperature at the hot end is presented in Fig. 6(d), in the figure, T_h is the temperature at the hot end of annular thermocouples, the maximum von Mises stress increases with the increase of the temperature at hot end of the annular thermocouples, the maximum von Mises stress of thermoelectric legs is larger than the yielding stress when θ=0.9, φ=6°. It means that too large temperature difference can lead to the maximum von Mises stress is larger than the yielding stress. And the maximum von Mises stress in the legs when θ=0.9 is higher than that in the legs when θ=0.7, especially when the temperature at hot end is larger than 100℃, thus, it is very necessary to optimize the structure parameters for extending the service life of annular thermocouples.

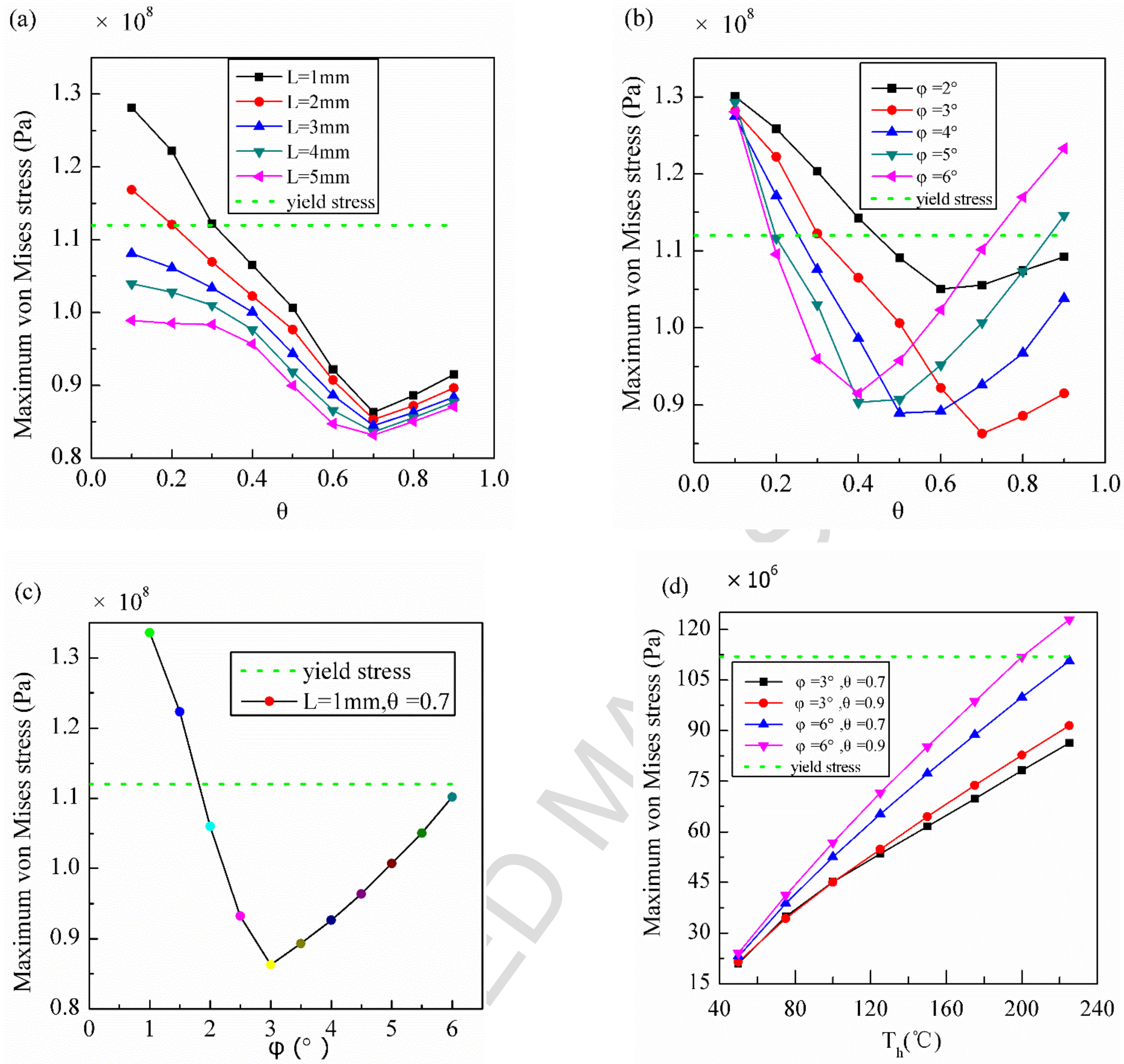

Fig.6 the effect of θ on the maximum von Mises stress in the leg of annular thermocouples, (a) φ=3° (b) L=1mm (c) the effect of φ on the maximum von Mises stress in the leg of annular thermocouple for θ=0.7 (d) the variation of the maximum von Mises stress with the temperature at the hot end when L=1mm

The von Mises stress nephogram in the legs of annular thermocouples is showed in Fig.7 when $L = 1\text{mm}, \theta = 0.7$, from the figure, it can be found that the maximum stress occurs in the contact area between the hot ends of the thermoelectric legs and the welding layer, which also is the easily destructive areas; the area of high stress level is gradually expanding with the increase of the total angle. And we note that the maximum von Mises stresses in the legs are 107MPa, 86.3MPa, 96.4MPa and 110MPa when the φ=1.5°, φ=3°, φ=4.5° and φ=6°, respectively, it is obviously the copper and welding layer have already produced the plastic deformation. The real stress level of thermoelectric legs should be lower than the simulated results because of the plastic deformation [22].

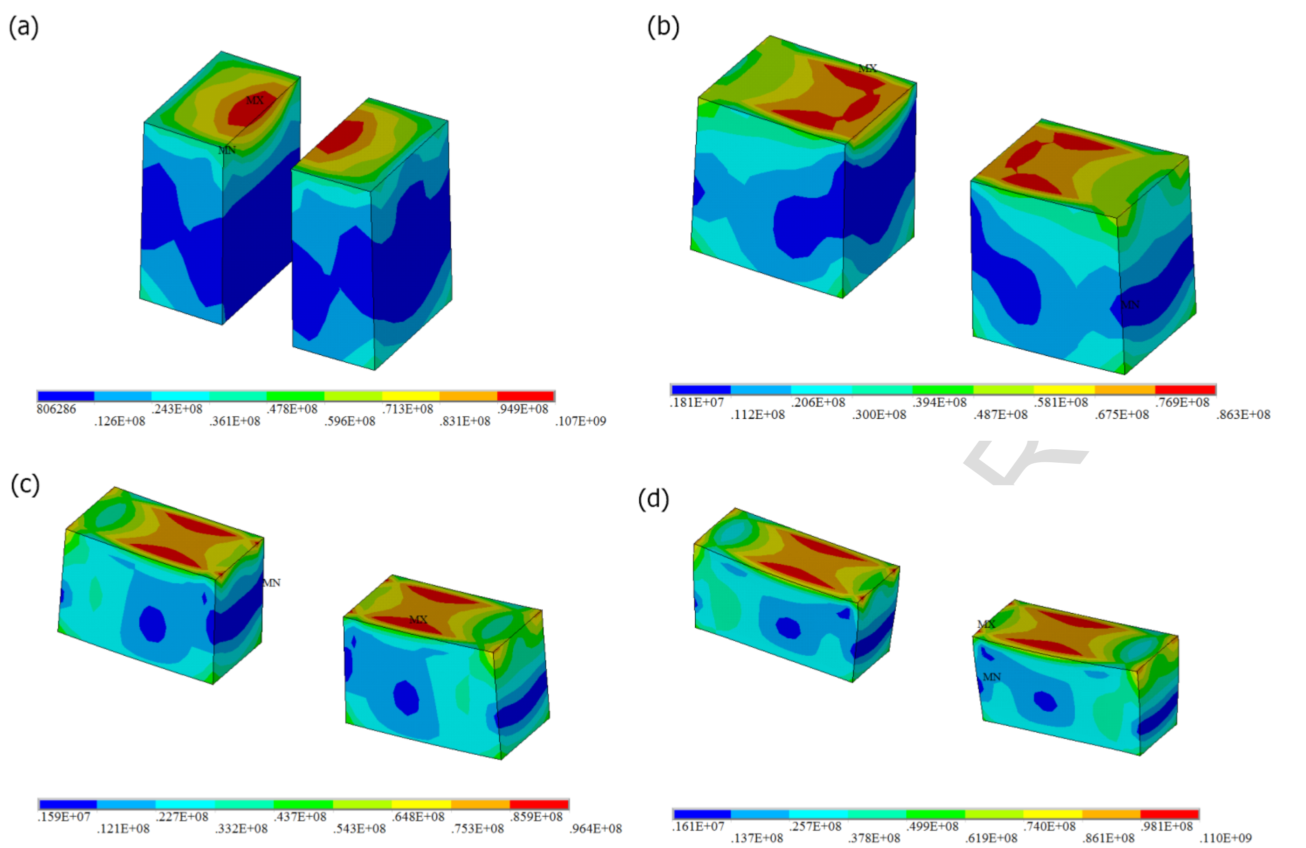

Fig.7 the von Mises stress (Pa) nephogram in the legs of annular thermocouples when $L = 1\text{mm}, \theta=0.7$. (a) $\varphi=1.5^\circ$ (b) $\varphi=3^\circ$ (c) $\varphi=4.5^\circ$ (d) $\varphi=6^\circ$.

All in all, in the practical application, the thermoelectric performance and mechanical reliability of annular thermocouples should be taken into account simultaneously. From above results discussed in Fig.5 and 6, that L=1mm , $\varphi=3^\circ$ and $\theta=0.7$ maybe a better choice as the structural parameters of annular thermocouples when both considering the thermoelectric performance and mechanical reliability.

3.3 The influence of the number of the thermocouples

The thermoelectric and mechanical performance of single annular thermocouples have been discussed in the above research, in the following calculations, we investigate the thermoelectric and mechanical performance of the whole annular thermoelectric generator, which is assembled from single annular thermocouples. Based on the above discussion, we choose L=1mm , $\varphi=3^\circ$ and $\theta = 0.75$ as the structural parameters of single annular thermocouple. In order to simplify the complexity of the simulation process, the annular thermocouples are uniformly distributed in the whole annular thermoelectric generator.

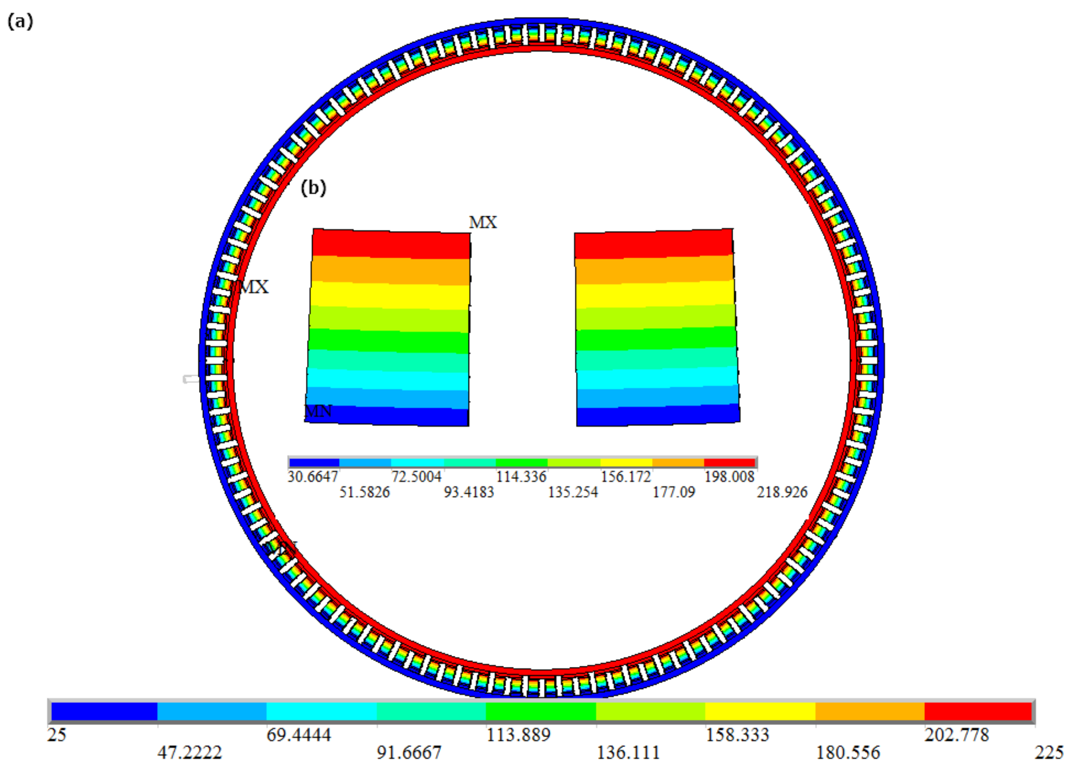

Fig.8 the temperature distribution nephogram in the annular thermoelectric generator (a) and its thermoelectric legs (b).

Fig.8 presents the temperature distribution nephogram in the annular thermoelectric generator (n=60, n stands for the number of the thermocouples in the annular thermoelectric generator). From the figure, it can be seen that the temperature distribution is symmetrical. And the temperature of ceramic plates is mainly equal to the temperature of the hot or cold sources because of the large thermal conductivity, while the considerable temperature contours are formed in the thermoelectric legs due to its low thermal conductivity and temperature dependent material properties.

The influence of the external load resistance on the thermoelectric performance of the annular thermoelectric generator for different n is showed in Fig. 9. From the Fig. 9 (a) and (b), it can be seen that the output power density and efficiency of the annular thermoelectric generator show a trend of first increase and then decrease with the increase of the external load resistance. The max efficiency is about 7.18%, 7.21%, 7.18% and 7.19% for $n=15$, $n=30$, $n=45$ and $n=60$, respectively, which means that the max efficiency is almost identical for any different n. Meanwhile, when the number n increases, the optimum external resistance for max output power density or conversion efficiency also increases, and when $R_L > 2.4\Omega$, the thermoelectric performance of annular thermoelectric generator of $n=60$ is higher than that of other cases.

Fig.10 presents the variation of the output power density and conversion efficiency of annular thermoelectric generator with the number of annular thermocouples for different R_L. In the figure, it can be seen that there is a max output power density or conversion efficiency by changing the number of thermocouples for different R_L. When the external load resistance increases, the optimum number of thermocouples for max output power density or conversion efficiency also increases. In addition, the max efficiency is about 7.08%, 7.29%, 7.21% and 7.26% for $R_L = 0.6$, $R_L = 1.2$, $R_L = 1.4$ and $R_L = 2.0$.

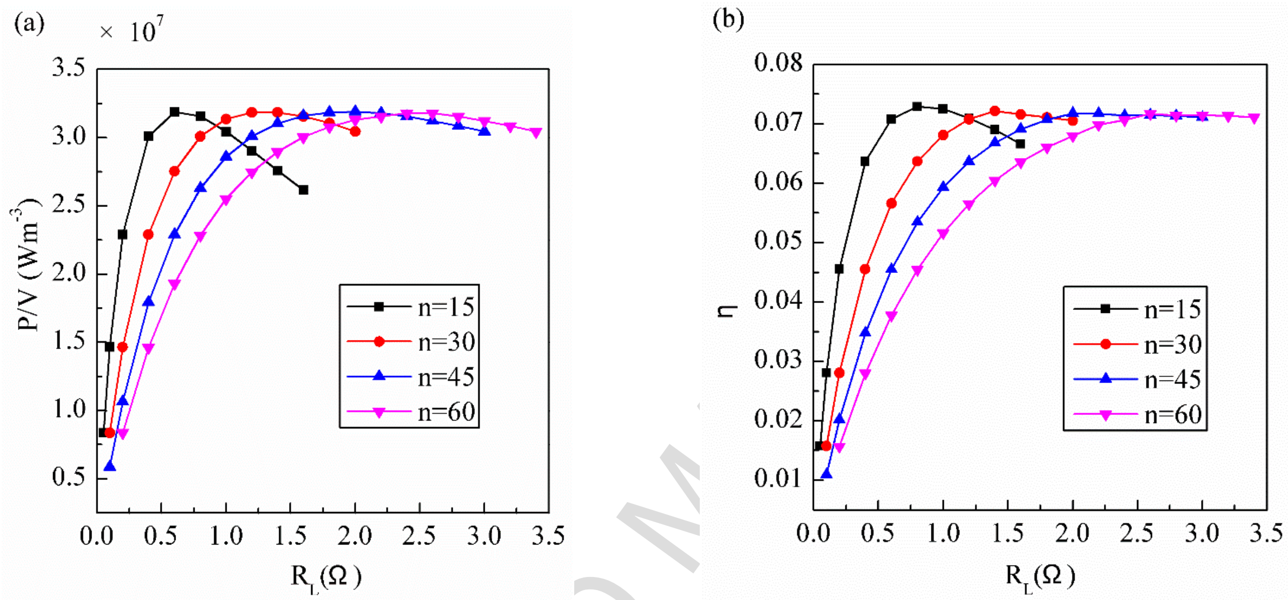

Fig.9 the influence of the external load resistance on the thermoelectric performance of the annular thermoelectric generator system, (a) the output power density (b) conversion efficiency

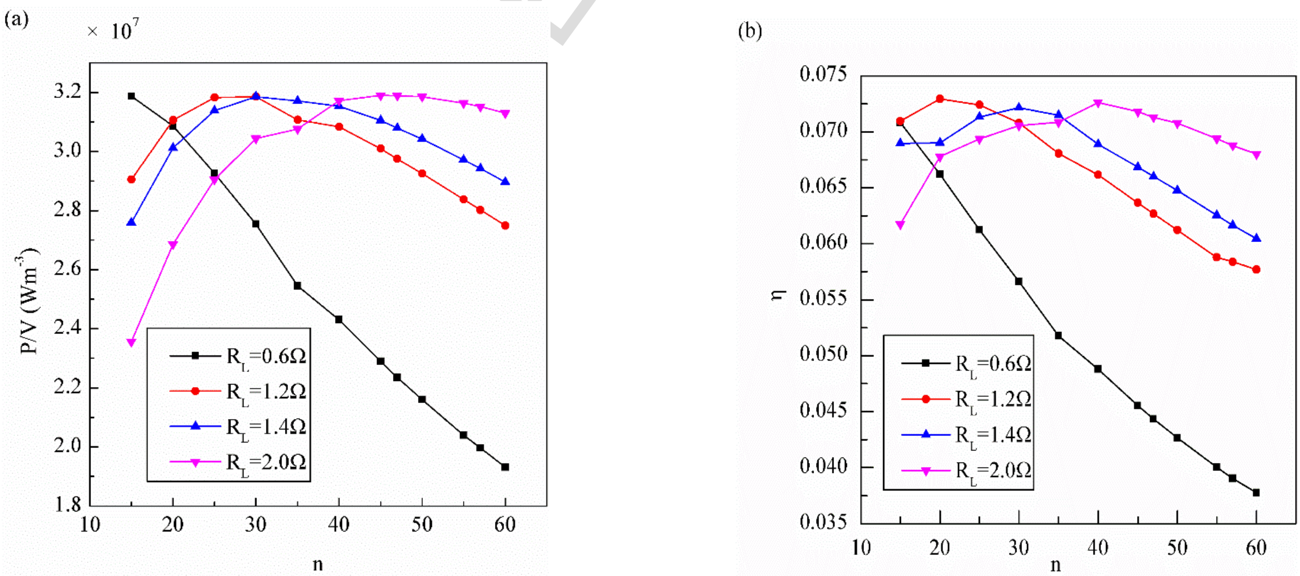

Fig.10 the influence of the number of thermocouples on the thermoelectric performance of the annular thermoelectric generator system, (a) the output power density (b) conversion efficiency

From the Fig.9 and 10, it is worth noting that the optimum number of the thermocouples is different for the different external load to improve the thermoelectric performance of the annular thermoelectric generator. Thus, in practical application, the appropriate annular thermoelectric devices should be selected according to the actual demand.

Fig.11 presents the influence of the number of thermocouples on the maximum von Mises stress in the leg of annular thermoelectric generators. From the figure, the influence of the number of thermocouples on the maximum von Mises stress is very small and irregular, the max difference of the stress value is 0.18MPa, which is only 0.2% of the minimum stress value in the numerical model.

The von Mises stress nephogram in the legs of annular thermoelectric generators when $n = 30$ and $n = 60$ is shown in Fig.12. From the figure, it can be seen that the distribution of von Mises stress contours and the low and high stress areas is similar in two cases. It shows that the mechanical reliability of the annular thermoelectric generator is mainly dependent on the geometric parameters of a single thermocouple, not the number of thermocouples in the whole annular thermoelectric generator.

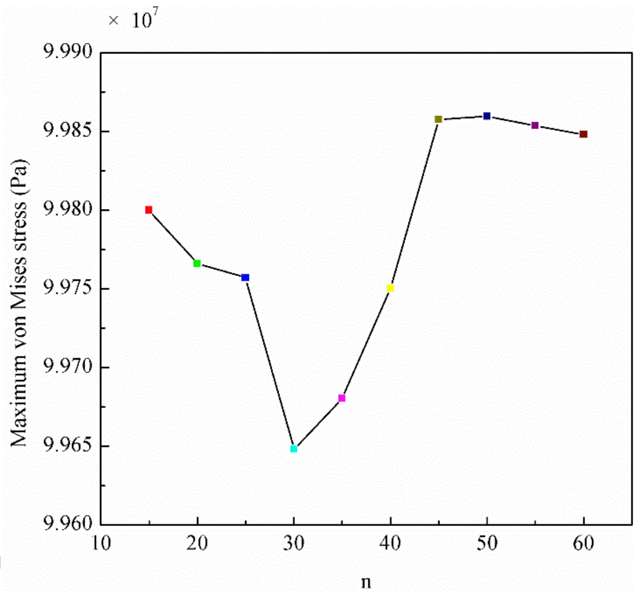

Fig.11 the influence of the number of thermocouples on the maximum von Mises stress in the leg of annular thermoelectric generators.

In summary, the appropriate annular thermoelectric devices should be selected according to the actual demand in practical application, and the number of the annular thermocouples has little influence on the mechanical reliability of the annular thermoelectric generator. The number of the annular thermocouples in the annular thermoelectric generator should choose $n = 60$ for improving the thermoelectric performance of the annular thermoelectric generator when the external load is enough large.

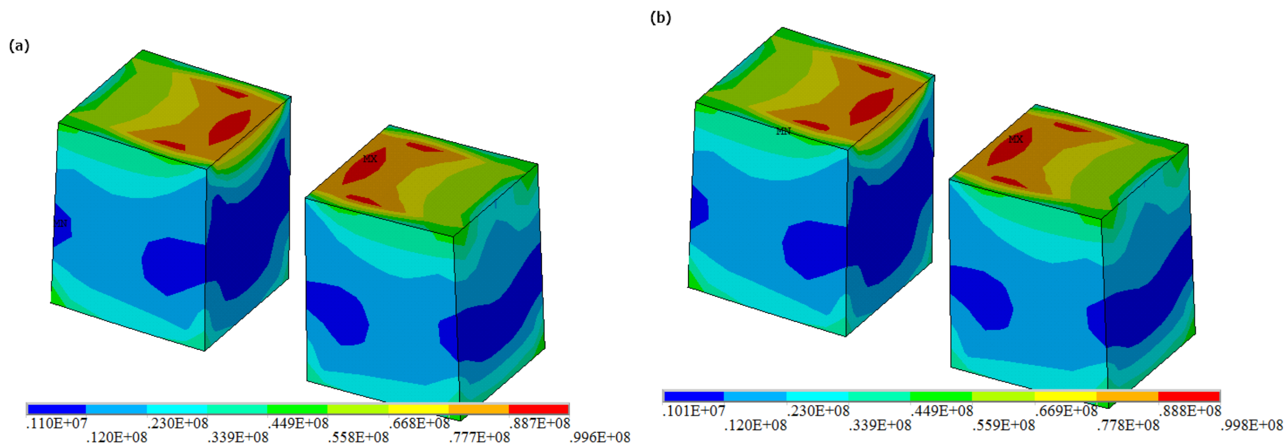

Fig.12 the von Mises stress nephogram in the legs of annular thermoelectric generator when L=1mm, (a) $n=30$ (b) $n=60$

4 Conclusion

The thermoelectric and thermal stress analyses of annular thermoelectric generators are investigated under steady conditions to optimize the geometric dimensions for improving the thermoelectric performance and mechanical reliability in this paper, the following conclusions can be obtained in the research.

(1) Increasing the length of the legs can improve the mechanical reliability, but reduce the thermoelectric performance of annular thermocouples.

(2) Increasing the angle ratio of the leg of annular thermocouples can improve the thermoelectric performance of the annular thermocouple, and there is an optimal angle ratio of legs for improving the mechanical reliability when the L and φ is fixed. In addition, changing the angle ratio of the legs, it can not only obtain the optimal value of the maximum von Mises stress, but also reduces the difference of the maximum von Mises stress between the annular thermocouples when the length of the legs is choose as 1mm and 5mm in our model.

(3) Increasing the total angle can improve the thermoelectric performance. From the Fig. 6(b) and (c), the maximum von Mises stress in the leg of annular thermocouples reaches the minimum when the θ=0.7, $\varphi=3^{\circ}$.

(4) The thermoelectric performance of the annular thermoelectric generator has a trend of first increase and then decrease with the increase of the number of annular thermocouples, which has little influence on the mechanical reliability of the annular thermoelectric generator.

(5) The optimal structural parameters (θ=0.7, $\varphi=3^{\circ}$ and L=1mm) of the annular thermocouple can be found for the improvement of thermoelectric performance and mechanical reliability. In this case, the optimal number of the annular thermocouples is 60 in the annular thermoelectric generator, which may improve the performance of the

annular thermoelectric generator.

This paper discussed the influences of the angle ratio of thermoelectric leg and the number of thermocouples on the thermoelectric performance and mechanical reliability, respectively. There is the existence of the optimal structure parameters for the annular thermoelectric generator with high thermoelectric and mechanical performance.

Acknowledgement

We are grateful for the grants from the National Natural Science Foundation of China (11572143, 11372120 and 11421062).

References

[1] Zheng X F, Yan Y Y, Simpson K. A potential candidate for the sustainable and reliable domestic energy generation–Thermoelectric cogeneration system [J]. Applied Thermal Engineering, 2013, 53(2): 305-311.

[2] Bell L E. Cooling, heating, generating power, and recovering waste heat with thermoelectric systems [J]. Science, 2008, 321(5895): 1457-1461.

[3] Bai S, Lu H, Wu T, et al. Numerical and experimental analysis for exhaust heat exchangers in automobile thermoelectric generators [J]. Case studies in thermal engineering, 2014, 4: 99-112.

[4] Chen G. Theoretical efficiency of solar thermoelectric energy generators [J]. Journal of Applied Physics, 2011, 109(10): 104908.

[5] Miao L, Kang Y P, Li C, et al. Experimental Performance of a Solar Thermoelectric Cogenerator Comprising Thermoelectric Modules and Parabolic Trough Concentrator without Evacuated Tube [J]. Journal of Electronic Materials, 2015, 44(6): 1972-1983.

[6] Baranowski L L, Warren E L, Toberer E S. High-temperature high-efficiency solar thermoelectric generators [J]. Journal of Electronic Materials, 2014, 43(6): 2348.

[7] Wu C. Analysis of waste-heat thermoelectric power generators [J]. Applied Thermal Engineering, 1996, 16(1): 63-69.

[8] Ali H, Yilbas B S, Al-Sulaiman F A. Segmented thermoelectric generator: Influence of pin shape configuration on the device performance [J]. Energy, 2016, 111: 439-452.

[9] Omer S A, Infield D G. Design and thermal analysis of a two stage solar concentrator for combined heat and thermoelectric power generation [J]. Energy conversion and management, 2000, 41(7): 737-756.

[10] Crane D T. An introduction to system-level, steady-state and transient modeling and optimization of high-power-density thermoelectric generator devices made of segmented thermoelectric elements [J]. Journal of Electronic Materials, 2011, 40(5): 561-569.

[11] Hadjistassou C, Kyriakides E, Georgiou J. Designing high efficiency segmented thermoelectric generators [J]. Energy conversion and management, 2013, 66: 165-172.

[12] Ibrahim A, Rahnamayan S, Martin M V, et al. Multi-objective thermal analysis of a thermoelectric device: Influence of geometric features on device characteristics [J]. Energy, 2014, 77: 305-317.

[13] Yilbas B S, Sahin A Z. Thermoelectric device and optimum external load parameter and slenderness ratio [J]. Energy, 2010, 35(12): 5380-5384.

[14] Sahin A Z, Yilbas B S. The thermoelement as thermoelectric power generator: effect of leg geometry on the efficiency and power generation [J]. Energy conversion and management, 2013, 65: 26-32.

[15] Liu Z, Zhu S, Ge Y, et al. Geometry optimization of two-stage thermoelectric generators using simplified conjugate-gradient method [J]. Applied Energy, 2017, 190: 540-552.

[16] Rezania A, Rosendahl L A, Yin H. Parametric optimization of thermoelectric elements footprint for maximum power generation

[J]. Journal of Power Sources, 2014, 255: 151-156.

[17] Kumar S, Heister S D, Xu X, et al. Thermoelectric generators for automotive waste heat recovery systems part ii: parametric evaluation and topological studies [J]. Journal of electronic materials, 2013, 42(6): 944.

[18] Yuan Z, Tang X, Liu Y, et al. A stacked and miniaturized radioisotope thermoelectric generator by screen printing [J]. Sensors and Actuators A: Physical, 2017, 267: 496-504.

[19] Manikandan S, Kaushik S C. Energy and exergy analysis of solar heat pipe based annular thermoelectric generator system [J]. Solar Energy, 2016, 135: 569-577.

[20] Shen Z G, Wu S Y, Xiao L. Theoretical analysis on the performance of annular thermoelectric couple[J]. Energy Conversion and Management, 2015, 89: 244-250.

[21] Kaushik S C, Manikandan S. The influence of Thomson effect in the energy and exergy efficiency of an annular thermoelectric generator [J]. Energy Conversion and Management, 2015, 103: 200-207.

[22] Erturun U, Erermis K, Mossi K. Effect of various leg geometries on thermo-mechanical and power generation performance of thermoelectric devices [J]. Applied Thermal Engineering, 2014, 73(1): 128-141.

[23] Wu Y, Ming T, Li X, et al. Numerical simulations on the temperature gradient and thermal stress of a thermoelectric power generator [J]. Energy Conversion and Management, 2014, 88: 915-927.

[24] Jia X, Gao Y. Estimation of thermoelectric and mechan ical performances of segmented thermoelectric generators under optimal operating conditions [J]. Applied Thermal Engineering, 2014, 73(1): 335-342.

[25] Gao J L, Du Q G, Zhang X D, et al. Thermal stress analysis and structure parameter selection for a Bi 2 Te 3-based thermoelectric module[J]. Journal of electronic materials, 2011, 40(5): 884-888.

[26] Erturun U, Erermis K, Mossi K. Influence of leg sizing and spacing on power generation and thermal stresses of thermoelectric devices [J]. Applied Energy, 2015, 159: 19-27.

[27] Erturun U, Mossi K. Thermoelectric devices with rotated and coaxial leg configurations: Numerical analysis of performance [J]. Applied Thermal Engineering, 2015, 85: 304-312.

[28] Al-Merbati A S, Yilbas B S, Sahin A Z. Thermodynamics and thermal stress analysis of thermoelectric power generator: influence of pin geometry on device performance [J]. Applied Thermal Engineering, 2013, 50(1): 683-692.

[29] Högblom O, Andersson R. Analysis of thermoelectric generator performance by Use of simulations and experiments [J]. Journal of Electronic Materials, 2014, 43(6): 2247-2254.

[30] Nye J F. Physical properties of crystals: their representation by tensors and matrices [M]. Oxford university press, 1985.

Highlights

1. The three dimension finite element model of annular thermoelectric devices is established.
2. The effect of geometric dimensions on the thermoelectric performance is discussed.
3. The mechanical reliability of annular thermoelectric devices is investigated
4. The optimal geometry dimensions of the annular thermoelectric generator are obtained.